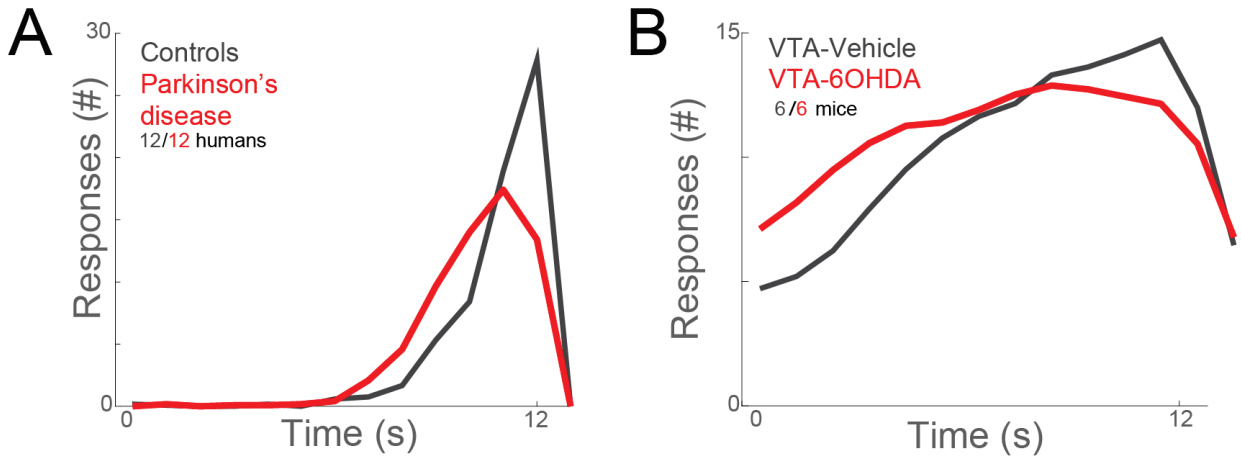

Figure S1. Related to Figure 1. Unnormalized response rate during interval timing for (A) human and (B) rodent data in Figure 1.

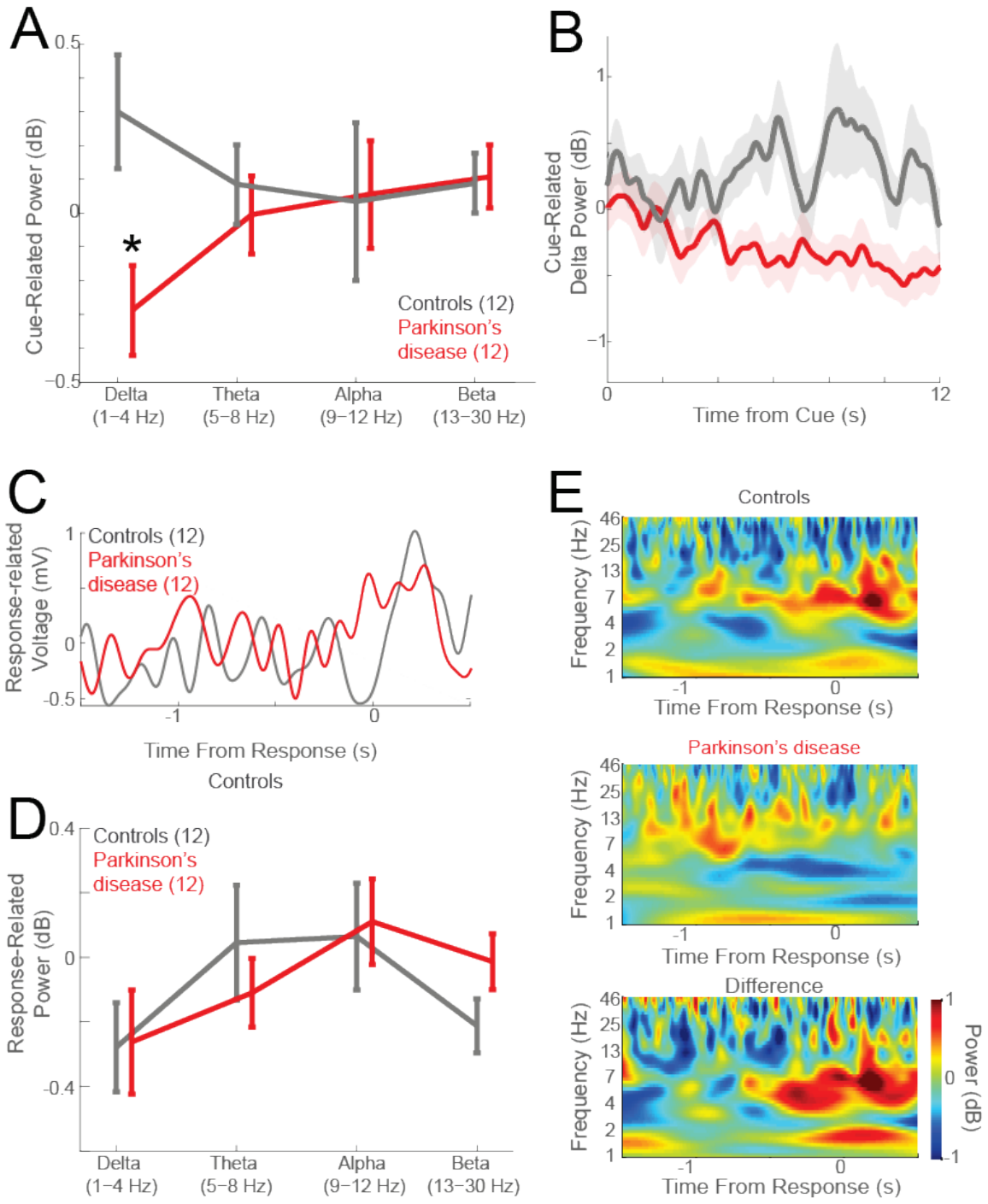

Figure S2. Related to Figure 1. **Cue-triggered MFC delta activity in PD during interval timing.** **(**A) Difference between control and PD patients in Figure 1 at electrode Cz during the interval (0 – 12 s); only consistent differences were found at delta bands (1-4 Hz). (B) Time evolution of delta power across the 12 s interval. Control – black; PD patients; red; * - indicates significance at $p < 0.05$. **(**C) Event-related potentials around responses from electrode Cz. (D) There were no consistent differences between controls and PD patients at any frequency bands in response-triggered activity. Control – black; PD patients; red. (E) Time-frequency plots of activity at electrode Cz around response revealed some delta and theta/beta modulation; however, this was not consistently different between control and PD patients.

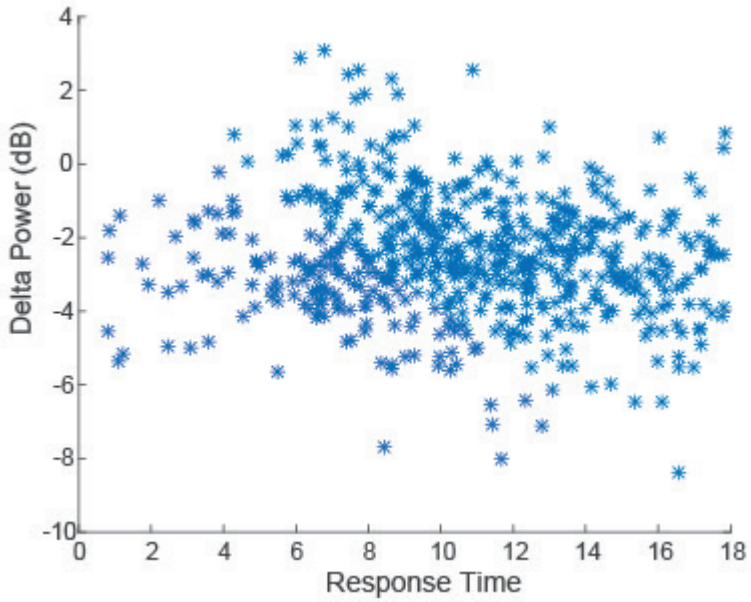

Figure S3. Related to Figure 1. **Delta power and time of responses during interval timing in mice**. We did not find a significant relationship between cue-triggered MFC delta power and when animals responded during interval timing.

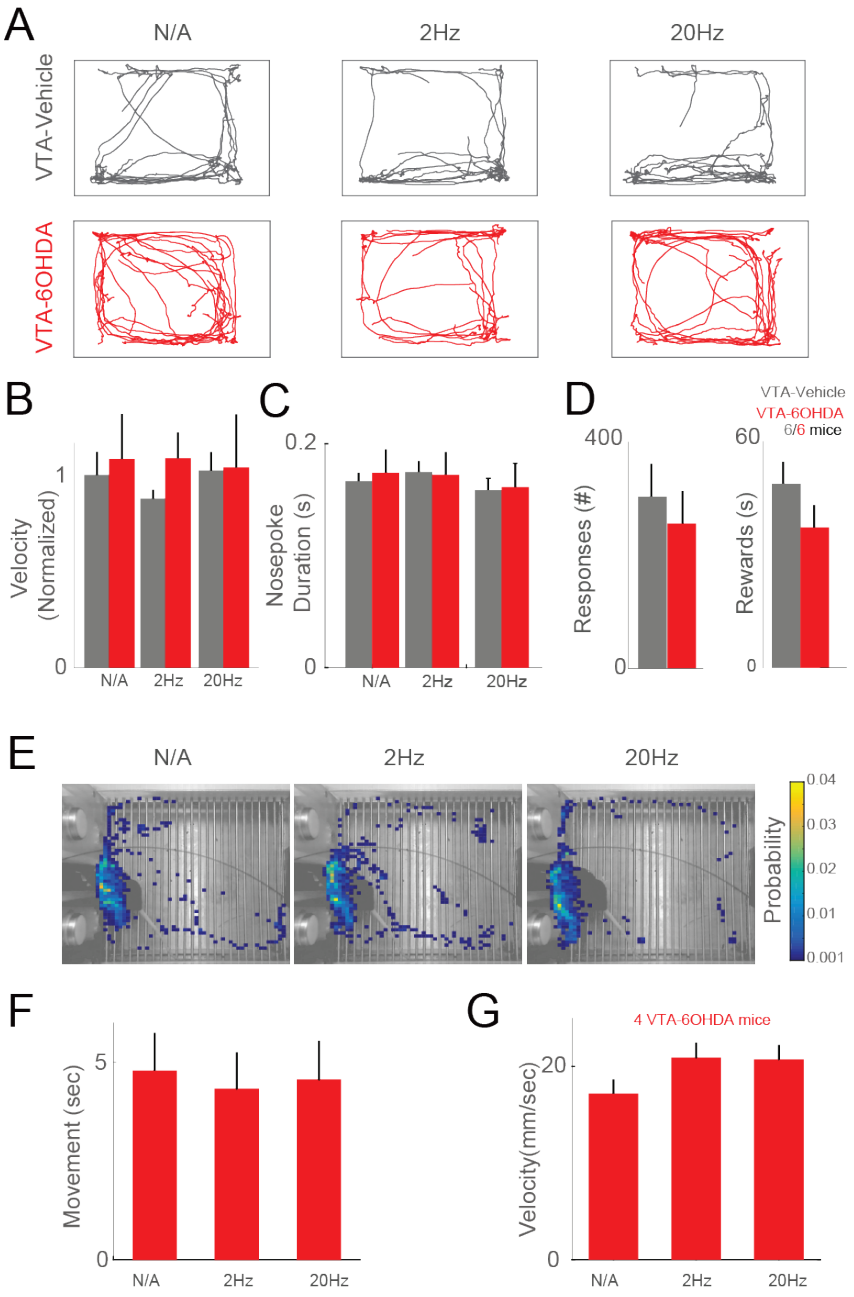

Figure S4. Related to Figure 5. **VTA-6OHDA, optogenetic stimulation, and movement.** (A) Open-field activity traces show similar pattern of movements in midbrain dopamine depleted animals with optogenetic stimulation. (B) There was no significant difference in average relative velocity of movement during open field testing over 30 minutes or C) nosepoke duration (the average amount of time the animals spent per nosepoke) in VTA-6OHDA mice or as a function of optogenetic stimulation at 2 or 20 Hz. D) Notably, we target the VTA which is distinct from animal models of motor aspects of PD which target the substantia nigra or the median forebrain bundle; VTA-6OHDA did not affect the number of responses, numbers of rewards. To further track movements, (E) we used the computer-vision toolbox in MATLAB to track animal position. Centroids of all animal positions were recorded plotted for VTA-6OHDA mice on interval timing trials with no stimulation and with 2 Hz stimulation and 20 Hz stimulation; each blue dot is a single pixel where animals spent >1 s; pixels in yellow are where animals spent the most time. (F) There was no consistent difference in overall movement or G) velocity of during interval timing as function of optogenetic stimulation in 4 VTA-6OHDA mice.

	Control	Parkinson's Disease	*P value*
N	12	12	
Age	63.4	64.7	*0.79*
R Handed	11	11	
Males	6	5	
MOCA	28.6	27.8	*0.19*
Education	15.7	15.3	*0.62*
LEDD		626	
UDPRS		11.5	

Table S1. Related to Figure 1. Patient demographic data; all of these patients were included in Parker et al., 2015 [S1] and 10 PD patients and 12 controls were included in Chen et., 2016 [S2].

Supplemental Experimental Procedures

Neurophysiological recordings

Freely moving electrophysiological recordings were performed as described in detail previously [S10,S13]. Mice were connected to recording head stages and cable without anesthesia. Neuronal ensemble recordings in the MFC were made using a multi-electrode recording system (Plexon). Raw wideband signal was high pass filtered at 0.05Hz with total gain of 5000 and recorded with 16bit digitization at 40k Hz sampling rate. To detect spikes, raw signals were re-referenced using common median referencing to minimize potential non-neural electrical noises and band-passed filtered between 300 and 6000 Hz offline. Spikes were detected with threshold of 5 median absolute deviations. Plexon Offline Sorter was used to sort single units and to remove artifacts. PCA and waveform shape were used for spike sorting. Single units were identified as having 1) consistent waveform shape, 2) separable clusters in PCA space, 3) a consistent refractory period of at least 1 ms in interspike interval histograms, and 4) consistent firing rates around behavioral events (as measured by a runs test of firing rates across trials around behavioral events; neurons with |z| scores > 4 were considered 'nonstationary' and were excluded). Unique neurons were verified by constructing two-dimensional cumulative distribution probabilities from Pearson's correlation coefficients of pair-wise waveform and interspike-interval comparisons and using a one-tailed threshold of $p<0.05$. Spike activity was analyzed for all cells that fired at rates above 0.1 Hz. Statistical summaries were based on all recorded neurons. No subpopulations were selected or filtered out of the neuron database. LFP was recorded with bandpass filters between 0.05 and 1000 Hz. Analysis of neuronal activity and quantitative analysis of basic firing properties were carried out with custom routines for MATLAB. All behavioral events and laser triggers were recorded simultaneously using TTL inputs at 40k Hz. Peri-event rasters and average histograms were constructed around trial start, and laser light pulse.

We analyzed our neuronal data according to procedures described at length previously [S1,S3–S10]. For each neuron, we constructed peri-event rasters using 0.01 bins from 0 – 12 s after trial start. We then calculated the mean peri-event firing rate from 0 to 12 s after trial start (FR_m) for each neuron. Next, we calculated the deviation in firing rate from FR_m at each bin over the 0-12 s epoch ($FR_i - FR_m$). These deviations were tested for normality via the Lilliefors test, and then normalized using z-scores according to the following formula:

$$\text{Zscore} = \frac{(FR_i - FR_m)}{SD_{fr}}$$

where, FR_i is the firing rate of *i*th bin of the peri-event period, FR_m is mean of firing rate from 0 to 12 s after trial start, SD_{fr} is the standard deviation of each bin's average firing rate of peri-event period. Population analyses of neuronal activity was tested for normality prior to further parametric statistical analysis.

We analyzed neuronal patterns using PCA, which we and others have widely used to identify patterns of neuronal activity in an unbiased, data-driven manner[S1,S9,S11]. PCA was constructed from z-transformed peri-event time histograms over the entire interval binned at 0.5 s and smoothed over 3 bins. The first bin was excluded to minimize the effects of stimulus-related modulation. All neurons from 12 mice with recordings (6 VTA-Vehicle/6 VTA-6OHDA) were included in PCA. The same PCs were projected onto putative MFC D1DR and untagged MFC neurons recorded from control mice (Fig 3) or for stimulated and unstimulated trials for untagged MFC neurons recorded from mice with VTA-6OHDA mice (Fig 4). For each comparison group (MFC D1DR vs. untagged MFC or stimulated vs. unstimulated trials in untagged MFC neurons) PC scores and normalized Euclidian distance in 3-dimensional PC space from the center of-mass of all PC scores were compared via a t-test[S12]. Ramping activity was also defined as neuronal activity that fit a linear model of firing rate over time across the interval using the function fitlm in matlab at $p<0.05$. Linear slope was calculated from neurons with a significant linear fit.

We quantified how neuronal ensembles encode timing using a naïve Bayesian classifier (fitNaiveBayes.m). Firing rates from untagged MFC neurons were grouped into 50ms bins, zscored, and smoothed over 424 ms using a Gaussian window. We used leave-one-out cross-validation to predict objective time from firing rate on stimulated vs. unstimulated trials. Shuffled data were generated by time-shuffling firing rate labels. Classification accuracy was quantified using R^2 of classifier-predicted vs. objective time. Classification performance was compared by testing correlation coefficients for significant differences using the cocor package in R using via Pearson-Filon z statistic [S13].

Mouse Interval Timing Task

Operant chambers (MedAssociates) were equipped with a nose poke hole with a yellow LED stimulus light (ENV-313W), a pellet dispenser (ENV-203-20), and a house light (ENV-315W). Behavioral arenas were housed in sound-attenuating chambers (MedAssociates). All behavioral responses including nose pokes and access to pellet receptacles were recorded with infra-red sensors. First, animals learned to make operant nose pokes to receive rewards (20-mg rodent purified pellets, F0071, BioServe). After fixed-ratio training, animals were trained in a 12 s fixed-interval timing task in which rewards were delivered for responses after a 12 s interval (Figure 1A). Early responses were not reinforced, which was distinct from the human version of the task. Responses between 12 and 18 s resulted in trial termination with reward delivery. Rewarded nose pokes were signaled by a house light. The house light was turned on at reward delivery and lasted until the animal collect the reward. Each trial was followed by a 24 ± 6s pseudorandom inter-trial interval which concluded with an 'on' nose poke hole light signaling the beginning of the next trial. All sessions were 60 minutes long. To examine effects of optogenetic stimulation during interval timing, a 720p camera was mounted on top of the operant chamber, and movement during the task was analyzed with the computer vision toolbox in MATLAB. The distribution of location, duration of movement, average velocity of movement during interval timing task was calculated for 2Hz, 20Hz stimulation trials as well as trials without stimulation.

Surgical procedures

Briefly, mice were anesthetized using ketamine (100 mg/kg) and xylazine (10 mg/kg). A surgical level of anesthesia was maintained with ketamine supplements (10 mg/kg) hourly (or as needed) with regular monitoring for stable respiratory rate and absent toe pinch response. Mice were placed in the stereotactic equipment with non-rupturing ear bars. A heating pad was used to prevent hypothermia. Under aseptic surgical conditions, the skull was leveled between bregma and lambda. A single craniotomy was drilled over the area above the MFC and two holes were drilled for skull screws. Virus injections were delivered with a 2 µL Hamilton syringe and 32 gauge needle injected at 0.1 µL/min. The injection needle was held at the injection site for 10 mins after injection and then slowly withdrawn. Vehicle (PBS and 0.03% ascorbic acid; pH 7.0) or 6OHDA (1 ug in 0.5 ul of 6OHDA dissolved in PBS and 0.03% ascorbic acid in each hemisphere; pH 7.0) was injected into the VTA of the medial midbrain (coordinates from bregma: AP: +3.3, ML ± 1.1, DV -4.6 at 10 degree angled) bilaterally. For optogenetic stimulation of MFC, a 200µm core optical fiber was implanted (coordinates from bregma: AP: +1.8, ML + 0.5, DV -1.5). For recording experiments, after injection of virus, a microelectrode array configured in 4x4 arrays of 50 µm stainless steel wires (200 µm between wires and rows; impedance measured in vitro at 400-600 kΩ; Microprobes) were implanted in animals (coordinates from bregma: AP: +1.8, ML + 0.5, DV -1.5). Electrode ground wires were wrapped around the skull screws. The electrode array was inserted while concurrently recording neuronal activity. The craniotomy was sealed with cyanoacrylate ('SloZap', Pacer Technologies) accelerated by 'ZipKicker' (Pacer Technologies), and methyl methacrylate (i.e., dental cement; AM Systems). Following implantation, animals recovered for two weeks before being reacclimatized to behavioral and recording procedures.

Time Frequency Analyses

Time-frequency calculations were computed using custom-written MATLAB routines described at length previously[S1,S4,S8,S9]. Time-frequency measures were computed by multiplying the fast Fourier transformed (FFT) power spectrum of LFP data with the FFT power spectrum of a set of complex Morlet wavelets (defined as a Gaussian-windowed complex sine wave: $e^{i2\pi tf}\, e^{-\frac{t^2}{2 \times \sigma^2}}$, where t is time, f is frequency (which increased from 1 to 50 Hz in 50 logarithmically spaced steps), and defines the width (or "cycles") of each frequency band, set according to $4/(2\pi f)$), and taking the inverse FFT. This time-domain signal convolution resulted in: 1) estimates of instantaneous power (the magnitude of the analytic signal), defined as Z[t] (power time series: $p(t) = real[z(t)]^2 + imag[z(t)]^2$); and, 2) phase (the phase angle) defined as = arctan(imag[z(t)]/real[z(t)]). Epochs were then cut in length surrounding the event of interest (-0.5 to +12 s). Power converted to a decibel (dB) scale (10*log10[power(t)/power(baseline)]) from a pre-stimulus baseline of -500 to -300 ms, allowing a direct comparison of effects across frequency bands. All statistical tests were hypothesis-driven t-test in delta (1-4 Hz) bands using a single bin over entire interval (0-12 s) based on our prior work.

Supplemental References

S1. Parker, K.L., Chen, K.-H., Kingyon, J.R., Cavanagh, J.F., and Naryanan, N.S. (2015). Medial frontal ~4 Hz activity in humans and rodents is attenuated in PD patients and in rodents with cortical dopamine depletion. J. Neurophysiol., jn.00412.2015.

S2. Chen, K.-H., Okerstrom, K.L., Kingyon, J.R., Anderson, S.W., Cavanagh, J.F., and Narayanan, N.S. (2016). Startle Habituation and Midfrontal Theta Activity in Parkinson's Disease. J Cogn Neurosci, 1–11.

S3. Allen, T.A., Narayanan, N.S., Kholodar-Smith, D.B., Zhao, Y., Laubach, M., and Brown, T.H. (2008). Imaging the spread of reversible brain inactivations using fluorescent muscimol. J. Neurosci. Methods *171*, 30–38.

S4. Narayanan, N.S., Cavanagh, J.F., Frank, M.J., and Laubach, M. (2013). Common medial frontal mechanisms of adaptive control in humans and rodents. Nat. Neurosci. *16*, 1888–1897.

S5. Narayanan, N.S., Rodnitzky, R.L., and Uc, E.Y. (2013). Prefrontal dopamine signaling and cognitive symptoms of Parkinson's disease. Rev Neurosci *24*, 267–278.

S6. Narayanan, N.S., and Laubach, M. (2009). Delay activity in rodent frontal cortex during a simple reaction time task. J. Neurophysiol *101*, 2859–2871.

S7. Narayanan, N.S., and Laubach, M. (2006). Top-down control of motor cortex ensembles by dorsomedial prefrontal cortex. Neuron *52*, 921–931.

S8. Parker, K.L., Ruggiero, R.N., and Narayanan, N.S. (2015). Infusion of D1 Dopamine Receptor Agonist into Medial Frontal Cortex Disrupts Neural Correlates of Interval Timing. Front Behav Neurosci *9*, 294.

S9. Parker, K.L., Chen, K.-H., Kingyon, J.R., Cavanagh, J.F., and Narayanan, N.S. (2014). D1-Dependent 4 Hz Oscillations and Ramping Activity in Rodent Medial Frontal Cortex during Interval Timing. J. Neurosci. *34*, 16774–16783.

S10. Narayanan, N.S., and Laubach, M. (2009). Methods for studying functional interactions among neuronal populations. Methods Mol. Biol *489*, 135–165.

S11. Chapin, J.K., and Nicolelis, M.A. (1999). Principal component analysis of neuronal ensemble activity reveals multidimensional somatosensory representations. J. Neurosci. Methods *94*, 121–140.

S12. Witten, I., and Frank, E. (2000). Data Mining (San Diego, CA: Academic Press).

S13. Diedenhofen, B., and Musch, J. (2015). cocor: A Comprehensive Solution for the Statistical Comparison of Correlations. PLoS ONE.